GEOPHYSICS, VOL. 63, NO. 6 (NOVEMBER-DECEMBER 1998); P. 1885–1897, 8 FIGS.

Magnetotelluric tensor decomposition: Part I, Theory for a basic procedure

F. E. M. (Ted) Lilley*

ABSTRACT

The problem of expressing a general 3-D magnetotelluric (MT) impedance tensor in the form of a 2-D tensor that has been distorted in some way is addressed first in terms of a general theorem. This theorem shows that when the real and quadrature parts of a tensor are analyzed separately as distinct matrices, all that is necessary to make a matrix with 2-D characteristics from one with 3-D characteristics is to allow the electric and magnetic observing axes to rotate independently.

The process is then examined in terms of the operations of twist and pure shear ("split") on such matrices. Both of two basic sequences of split after twist, and twist after split, produce a typical 3-D matrix from one initially 1-D, with the parameters of split contributing 2-D characteristics to the final matrix. Taken in reverse, these sequences offer two basic paths for the decomposition of a 3-D matrix, and are seen to be linked to the initial theorem.

The various operations on matrices are expressed diagrammatically using the Mohr circle construction, of which it is demonstrated two types are possible. Mohr circles of an observed MT tensor display all the information held by the tensor, and the two types of circle construction respectively make clear whether particular data are well suited to modeling by either split after twist, or twist after split. Generally, tensor decompositions may be displayed by charting their progress in Mohr space.

The Mohr construction also displays the invariants of a tensor and shows that tensor decomposition can be viewed as a process of determining an appropriate set of invariants. An expectation that the origin of axes should be outside every circle categorizes as irregular any tensors which, in either the real or quadrature part, do not satisfy a $Z_{xy}Z_{yx} < Z_{xx}Z_{yy}$ criterion.

The theory of the present paper applies equally to procedures for distorting 1-D and 2-D model calculations for the purpose of matching observed 3-D data.

INTRODUCTION

This paper presents a procedure for the decomposition of a 3-D tensor into 2-D form at a basic level. Such an exercise is a valuable introduction to, and lays a firm foundation for, the use of more sophisticated decomposition techniques. But more than this, information is obtained which is useful as a benchmark in comparison with more sophisticated methods. Do they actually perform as well? Do they obtain their results so clearly? Are their assumptions justified?

Although based on algebraic analysis, the strategy followed comes strongly from insight gained from graphical tensor representation, using the Mohr construction. The use of Mohr circles has been valuable in structural geology, as described by DePaor and Means (1984) and Means (1990, 1992, 1994). Especially from this source have come basic concepts applied in this paper: a general 3-D magnetotelluric (MT) matrix being reducible to a twist acting on a splitting operator or a splitting operator acting on a twist (the terms "split" and "twist" are defined explicitly later in this paper). It will be clear also that I have been led into such considerations by the analysis of Groom and Bailey (1989) and by the series of papers comprising Bahr (1988, 1991), Chakridi et al. (1992), Chave and Smith (1994), and Smith (1995).

The procedure of the present paper analyzes an MT tensor in terms of its real and quadrature matrices taken separately. Readers who work with apparent resistivity and phase will find the present parameters less familiar; however, transfer from one set to the other is direct. It is appropriate to recognize that though in instances (such as when calculating the Fourier transform of a time series) the partition between real and quadrature parts may depend on a time taken arbitrarily for the start of the transform, in MT analysis the real and quadrature parts of the tensor are geology dependent, not time-series dependent.

Manuscript received by the Editor December 23, 1996; revised manuscript received May 14, 1998.
*Research School of Earth Sciences, Australian National University, Canberra, A.C.T. 0200, Australia. E-mail: Ted.Lilley@anu.edu.au.

Initially, a basic theorem will be stated, that if the electric (E) and magnetic (H) measuring axes are allowed to rotate independently, the matrix for the real part of a general observed MT tensor can be expressed immediately in 2-D form. Allowing different and independent rotations of the (E) and (H) measuring axes, the matrix for the quadrature part of the tensor can also be expressed in 2-D form. The parameters of these 2-D forms, and the axis rotations which produce them, recur throughout the paper.

Then, the existence of the two kinds of Mohr circles of DePaor and Means (1984) will be demonstrated for MT data. It will be shown how these are valuable in displaying where "twist" and "split" come into matrix distortion.

Two basic models for MT tensor distortion are examined, involving matrices of 1-D, 2-D, and 3-D form. The first model for a 3-D matrix comprises a 1-D matrix upon which a twist operates, and then a split. The second model comprises a 1-D matrix upon which a split operates, followed by a twist. In each case, the split contributes 2-D characteristics. Starting from a different formal basis, the models produce the results of the initial introductory theorem.

The following notation is adopted throughout this paper for the MT tensor: **Z** denotes the impedance tensor with axes in some particular orientation (for example, either aligned north and east, or aligned parallel and perpendicular to geologic strike); **Z**′ denotes the impedance tensor after some form of axis rotation.

In treating in this paper the real and quadrature matrices of an MT tensor generally separately, subscripts which could denote real and quadrature parts are omitted from much of the text. To illustrate the use of this convention, equations (19) and (20) below, as examples, may be considered to have the two "modes" of real and quadrature. In the real mode, the matrix of the real parts of the tensor elements is taken, and used to solve for values for θ_e and θ_h for the real part of the tensor (where θ_e and θ_h are rotation angles for the electric and magnetic axes, respectively). In the quadrature mode, the (real) matrix of the quadrature parts of the tensor elements is taken, and used to solve for values for θ_e and θ_h for the quadrature part of the tensor.

At the end of such an analysis, and as shown in the examples of a companion paper (Lilley, 1998), results are compared which have been obtained from pursuing both the real and quadrature modes of analysis separately. At this stage also, the real and quadrature results may be recombined, where there is justification for doing so, in carrying the now-decomposed tensor forward for interpretation. For example, a mean may be formed from real and quadrature strike determinations; complex principal impedances may be formed by taking real and quadrature pairs of principal values.

Another point to make in this introduction is that there is commonly an ambiguity of 90° in the determinations of geologic strike direction in this paper. In what follows, this point will be taken as understood and not repeated. The ambiguity arises because when axes are rotated to achieve an ideal 2-D form for a tensor, as in equation (12) below, there is no indication from the MT data alone which axis direction is along strike and which is across strike. Strike direction thus has a 90° ambiguity.

A BASIC THEOREM

The theorem

Much of the following paper is concerned with traditional tensor rotation, when the orthogonal measuring axes are rotated in a simple way. First, however, it is instructive to remember a basic theorem, which shows that if the measuring axes for E and H are allowed to rotate independently, as in Figure 1a, the real (or, alternatively the quadrature) part of any general observed tensor may be immediately reduced to 2-D form. The essence of this theorem may be found in Larsen (1975) and Cox et al. (1980), and a variation of it is discussed by Pedersen (1988). In the form where the same rotations are sought for both real and quadrature, it is applied, for example, by Ferguson (1988) to the "deskewing" of seafloor MT data subsequently described by Ferguson et al. (1990).

Let the original tensor, with observation axes oriented traditionally north and east, be

$$\begin{bmatrix} Z_{xxr} + iZ_{xxq} & Z_{xyr} + iZ_{xyq} \\ Z_{yxr} + iZ_{yxq} & Z_{yyr} + iZ_{yyq} \end{bmatrix} \quad (1)$$

where subscripts r and q denote real and quadrature and, for the purposes of examining this tensor, assume a linearly polarised and horizontal magnetic field which is entirely

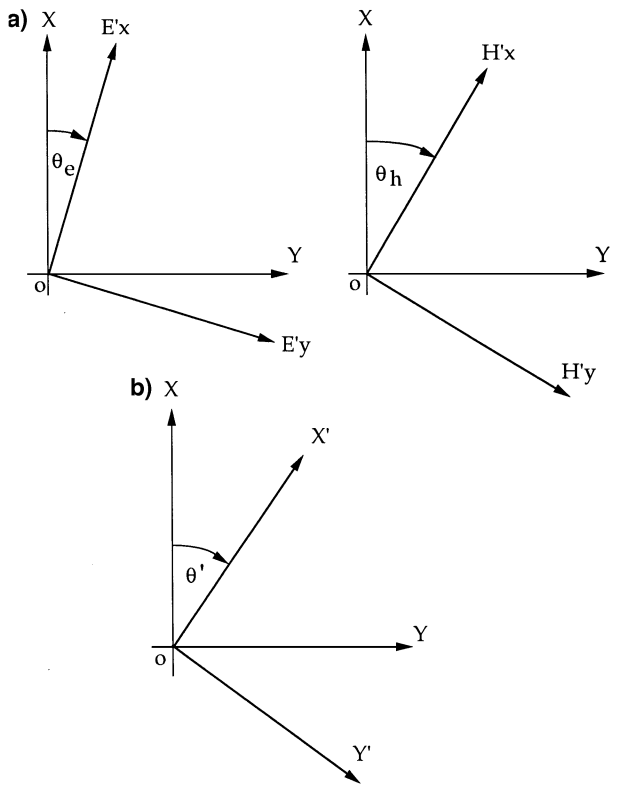

FIG. 1. Geometry for rotation of measuring axes. (a) The case for the basic theorem, where the E axes are rotated angle θ_e, and the H axes are rotated angle θ_h. (b) The common case, where the measuring axes XOY are rotated angle θ' clockwise to $X'OY'$ for both E and H fields.

"in-phase." Then, the electric and magnetic fields obey

$$\begin{bmatrix} E_{xr} + iE_{xq} \\ E_{y_r} + iE_{y_q} \end{bmatrix} = \begin{bmatrix} Z_{xxr} + iZ_{xxq} & Z_{xy_r} + iZ_{xy_q} \\ Z_{yx_r} + iZ_{yx_q} & Z_{yy_r} + iZ_{yy_q} \end{bmatrix} \begin{bmatrix} H_{xr} \\ H_{y_r} \end{bmatrix}, \tag{2}$$

which, writing the equations for the real and quadrature parts separately, gives

$$\begin{bmatrix} E_{xr} \\ E_{y_r} \end{bmatrix} = \begin{bmatrix} Z_{xxr} & Z_{xy_r} \\ Z_{yx_r} & Z_{yy_r} \end{bmatrix} \begin{bmatrix} H_{xr} \\ H_{y_r} \end{bmatrix} \tag{3}$$

and

$$\begin{bmatrix} E_{xq} \\ E_{y_q} \end{bmatrix} = \begin{bmatrix} Z_{xxq} & Z_{xy_q} \\ Z_{yx_q} & Z_{yy_q} \end{bmatrix} \begin{bmatrix} H_{xr} \\ H_{y_r} \end{bmatrix}. \tag{4}$$

Adopting now the convention of omitting r and q subscripts allows both equations (3) and (4) to be represented by equation (5) below, and the real and quadrature parts of the tensor then examined separately. Thus, for the matrix of either the real or quadrature tensor elements, we have:

$$\begin{bmatrix} E_x \\ E_y \end{bmatrix} = \begin{bmatrix} Z_{xx} & Z_{xy} \\ Z_{yx} & Z_{yy} \end{bmatrix} \begin{bmatrix} H_x \\ H_y \end{bmatrix}. \tag{5}$$

Now consider the electric and magnetic fields to be measured by axes rotated clockwise through angles θ_e and θ_h, respectively, as shown in Figure 1a. Then, equation (5) may be written

$$\begin{bmatrix} E'_x \\ E'_y \end{bmatrix} = \begin{bmatrix} \cos\theta_e & \sin\theta_e \\ -\sin\theta_e & \cos\theta_e \end{bmatrix} \begin{bmatrix} Z_{xx} & Z_{xy} \\ Z_{yx} & Z_{yy} \end{bmatrix} \times \begin{bmatrix} \cos\theta_h & -\sin\theta_h \\ \sin\theta_h & \cos\theta_h \end{bmatrix} \begin{bmatrix} H'_x \\ H'_y \end{bmatrix}, \tag{6}$$

that is,

$$\begin{bmatrix} E'_x \\ E'_y \end{bmatrix} = \begin{bmatrix} Z'_{xx} & Z'_{xy} \\ Z'_{yx} & Z'_{yy} \end{bmatrix} \begin{bmatrix} H'_x \\ H'_y \end{bmatrix}, \tag{7}$$

where

$$Z'_{xx} = Z_{xx}\cos\theta_e\cos\theta_h + Z_{xy}\cos\theta_e\sin\theta_h + Z_{yx}\sin\theta_e\cos\theta_h + Z_{yy}\sin\theta_e\sin\theta_h, \tag{8}$$

$$Z'_{xy} = -Z_{xx}\cos\theta_e\sin\theta_h + Z_{xy}\cos\theta_e\cos\theta_h - Z_{yx}\sin\theta_e\sin\theta_h + Z_{yy}\sin\theta_e\cos\theta_h, \tag{9}$$

$$Z'_{yx} = -Z_{xx}\sin\theta_e\cos\theta_h - Z_{xy}\sin\theta_e\sin\theta_h + Z_{yx}\cos\theta_e\cos\theta_h + Z_{yy}\cos\theta_e\sin\theta_h, \tag{10}$$

$$Z'_{yy} = Z_{xx}\sin\theta_e\sin\theta_h - Z_{xy}\sin\theta_e\cos\theta_h - Z_{yx}\cos\theta_e\sin\theta_h + Z_{yy}\cos\theta_e\cos\theta_h. \tag{11}$$

Equation (7) is of the form

$$\begin{bmatrix} E'_x \\ E'_y \end{bmatrix} = \begin{bmatrix} 0 & Z^P_{xy} \\ -Z^P_{yx} & 0 \end{bmatrix} = \begin{bmatrix} H'_x \\ H'_y \end{bmatrix} \tag{12}$$

when, in equations (8) to (11), the following relationships hold:

$$Z_{xx}\cos\theta_e\cos\theta_h + Z_{xy}\cos\theta_e\sin\theta_h + Z_{yx}\sin\theta_e\cos\theta_h + Z_{yy}\sin\theta_e\sin\theta_h = 0, \tag{13}$$

$$-Z_{xx}\cos\theta_e\sin\theta_h + Z_{xy}\cos\theta_e\cos\theta_h - Z_{yx}\sin\theta_e\sin\theta_h + Z_{yy}\sin\theta_e\cos\theta_h = Z^P_{xy}, \tag{14}$$

$$-Z_{xx}\sin\theta_e\cos\theta_h - Z_{xy}\sin\theta_e\sin\theta_h + Z_{yx}\cos\theta_e\cos\theta_h + Z_{yy}\cos\theta_e\sin\theta_h = -Z^P_{yx}, \tag{15}$$

$$Z_{xx}\sin\theta_e\sin\theta_h - Z_{xy}\sin\theta_e\cos\theta_h - Z_{yx}\cos\theta_e\sin\theta_h + Z_{yy}\cos\theta_e\cos\theta_h = 0. \tag{16}$$

In equation (12), the quantity Z^P_{yx} is defined with a coefficient of -1 so that in an actual example the numerical values of both Z^P_{xy} and Z^P_{yx} will be positive in sign. In this paper, Z^P_{xy} and Z^P_{yx} are termed the "principal values" of the MT matrix in equation (5).

Rotation parameters and principal values

In the above equations, adding equations (13) and (16) gives

$$\tan(\theta_e - \theta_h) = \frac{Z_{yy} + Z_{xx}}{Z_{xy} - Z_{yx}}, \tag{17}$$

whereas subtracting equation (13) from equation (16) gives

$$\tan(\theta_e + \theta_h) = \frac{Z_{yy} - Z_{xx}}{Z_{xy} + Z_{yx}}, \tag{18}$$

whence

$$\theta_e = \frac{1}{2}\left[\arctan\frac{Z_{yy} - Z_{xx}}{Z_{xy} + Z_{yx}} + \arctan\frac{Z_{yy} + Z_{xx}}{Z_{xy} - Z_{yx}}\right] \tag{19}$$

and

$$\theta_h = \frac{1}{2}\left[\arctan\frac{Z_{yy} - Z_{xx}}{Z_{xy} + Z_{yx}} - \arctan\frac{Z_{yy} + Z_{xx}}{Z_{xy} - Z_{yx}}\right]. \tag{20}$$

Similarly, adding equations (14) and (15) gives

$$Z^P_{xy} - Z^P_{yx} = \cos(\theta_e + \theta_h)[(Z_{yx} + Z_{xy}) + \tan(\theta_e + \theta_h)(Z_{yy} - Z_{xx})], \tag{21}$$

whereas subtracting equation (15) from equation (14) gives

$$Z^P_{xy} + Z^P_{yx} = \cos(\theta_e - \theta_h)[(Z_{yx} - Z_{xy}) - \tan(\theta_e - \theta_h)(Z_{yy} + Z_{xx})]. \tag{22}$$

Squaring these two equations, substituting for $\tan(\theta_e - \theta_h)$ and $\tan(\theta_e + \theta_h)$ from equations (17) and (18), and using

$$\cos^2\nu = \frac{1}{\tan^2\nu + 1} \tag{23}$$

for general angle ν, then allows their simplification to

$$Z^P_{xy} - Z^P_{yx} = \pm\left[(Z_{yy} - Z_{xx})^2 + (Z_{xy} + Z_{yx})^2\right]^{\frac{1}{2}} \tag{24}$$

and

$$Z^P_{xy} + Z^P_{yx} = \pm\left[(Z_{yy} + Z_{xx})^2 + (Z_{yx} - Z_{xy})^2\right]^{\frac{1}{2}}. \tag{25}$$

From equations (24) and (25), it follows that

$$Z^P_{xy} = \tfrac{1}{2}\Big\{\left[(Z_{yy} + Z_{xx})^2 + (Z_{yx} - Z_{xy})^2\right]^{\frac{1}{2}} - \left[(Z_{yy} - Z_{xx})^2 + (Z_{xy} + Z_{yx})^2\right]^{\frac{1}{2}}\Big\} \tag{26}$$

and

$$Z^P_{yx} = \tfrac{1}{2}\Big\{\left[(Z_{yy} + Z_{xx})^2 + (Z_{yx} - Z_{xy})^2\right]^{\frac{1}{2}} + \left[(Z_{yy} - Z_{xx})^2 + (Z_{xy} + Z_{yx})^2\right]^{\frac{1}{2}}\Big\}, \tag{27}$$

where the sign options arising from the square roots are taken so that Z^P_{xy} and Z^P_{yx} are both positive, with Z^P_{yx} the greater of the two.

Interpretation

The observed four parameters, Z_{xx}, Z_{xy}, Z_{yx}, and Z_{yy}, have been cast into the four different parameters of a skewed 2-D model: θ_e, θ_h, Z^P_{xy}, and Z^P_{yx}. These latter parameters can be determined directly, and plotted as functions of frequency, for both real and quadrature modes. Examples are given in the companion paper (Lilley, 1998).

An elementary interpretation of these data, to some extent intuitive and to some extent based on practical experience, is that the rotated E-field axes will indicate local geologic strike, whereas the rotated H-field axes indicate regional geologic strike (if, indeed, concepts of geologic strike, with their implications of 2-D structure, are justified locally or regionally).

Arguments for the E-axis interpretation are typically based on the common experience that highly conductive structure of the same length scale as the E-field measuring apparatus will "clamp" its strike direction on the observations, over all frequencies. Arguments for the H-field axis interpretation are typically that because the magnetic fields represent an integration over volume, the magnetic strike will be a bulk or regional effect.

The latter argument, by itself, occurs extensively in magnetovariational studies, where real and quadrature Parkinson arrows (also called induction vectors, or "tippers"), are commonly taken to be perpendicular to regional strike, and thus used to determine regional strike direction. If real and quadrature arrows are not parallel, their mean direction may be used, and their difference taken as an indicator of departure from two dimensionality.

Always, in an interpretation in terms of the parameters θ_e, θ_h, Z^P_{xy}, and Z^P_{yx}, the extent of period independence of θ_e and θ_h is significant, as is the extent of their agreement between real and quadrature modes. Justification of the 2-D analysis given above is stronger the more such period independence exists, and the more the real and quadrature modes are in agreement.

GENERAL ROTATION OF AXES, AND GENERATION OF MOHR CIRCLES

Traditional axis rotation

Returning now to the traditional situation, the E and H observing axes are rotated together, say clockwise through θ', as shown in Figure 1b. Then in equation (6),

$$\begin{bmatrix} E'_x \\ E'_y \end{bmatrix} = \begin{bmatrix} \cos\theta' & \sin\theta' \\ -\sin\theta' & \cos\theta' \end{bmatrix} \begin{bmatrix} Z_{xx} & Z_{xy} \\ Z_{yx} & Z_{yy} \end{bmatrix} \times \begin{bmatrix} \cos\theta' & -\sin\theta' \\ \sin\theta' & \cos\theta' \end{bmatrix} \begin{bmatrix} H'_x \\ H'_y \end{bmatrix}. \tag{28}$$

Equation (12) no longer holds (except for ideal 2-D data), and equations (8) to (11) take the form

$$Z'_{xx} = (Z_{xx} + Z_{yy})/2 + C\sin(2\theta' + \beta), \tag{29}$$

$$Z'_{xy} = (Z_{xy} - Z_{yx})/2 + C\cos(2\theta' + \beta), \tag{30}$$

$$Z'_{yx} = -(Z_{xy} - Z_{yx})/2 + C\cos(2\theta' + \beta), \tag{31}$$

$$Z'_{yy} = (Z_{xx} + Z_{yy})/2 - C\sin(2\theta' + \beta), \tag{32}$$

where

$$C = \tfrac{1}{2}\left[(Z_{xx} - Z_{yy})^2 + (Z_{xy} + Z_{yx})^2\right]^{\frac{1}{2}} \tag{33}$$

and β is defined by

$$\tan\beta = \frac{Z_{xx} - Z_{yy}}{Z_{xy} + Z_{yx}}. \tag{34}$$

It is useful to introduce an auxiliary angle β', expressed as

$$\tan\beta' = \frac{Z'_{xx} - Z'_{yy}}{Z'_{xy} + Z'_{yx}}, \tag{35}$$

which enables θ' to be expressed as

$$\theta' = \tfrac{1}{2}(\beta' - \beta). \tag{36}$$

Also, it is useful to define an angle γ, as

$$\tan\gamma = \frac{Z_{yy} + Z_{xx}}{Z_{xy} - Z_{yx}}. \tag{37}$$

Although in this section, separate E and H axis rotations have not been implemented, the parameters θ_e and θ_h stand defined by equations (19) and (20) and, in terms of these, note

that β and γ may be expressed as

$$\beta = -(\theta_e + \theta_h) \tag{38}$$

and

$$\gamma = \theta_e - \theta_h. \tag{39}$$

Equation (38) is given by adding equations (19) and (20) and invoking equation (34); equation (39) is given by subtracting equations (19) and (20) and invoking equation (37).

Mohr circles: two types

The form of the equations (29) to (32) allows the process of axes rotation by angle θ' to be depicted diagrammatically as Mohr circles (Lilley, 1976, 1993a), of which two types are possible (DePaor and Means, 1984), as shown in Figure 2. Both circles are of radius C. Starting from the observed (Z_{xy}, Z_{xx}) or (Z_{xy}, Z_{yy}) data pair (as marked in the figure), rotation of the radial arm by angle $2\theta'$ takes one around both circles to the other (Z'_{xy}, Z'_{xx}) or (Z'_{xy}, Z'_{yy}) data pairs possible as a result of axes rotation by angle θ'.

The two types of circle have some different properties. In earlier papers, I used type 1 circles.

For both types of circles, two dimensionality of the tensor causes the two horizontal axes, for Z'_{xy} and Z'_{yx}, to be superimposed because $(Z_{xx} + Z_{yy})$ is zero. The circle center is then on a single horizontal axis. An example of 2-D data, from the PNG data set distributed for the second MT Data Interpretation Workshop (MTDIW2; Jones and Schultz, 1997), is shown in Figure 3.

For one dimensionality, $C = 0$, and the circles of both kinds reduce to their central points. Lilley (1993a) examines the form the circles (of the first type) will take for some special cases, of strong tensor anisotropy, etc. Lilley (1993b) examines the form such circles will take in the case of 2-D "static shift" (in fact, the circles in Figure 3 have this form to the extent that all circles lie in a common envelope formed by two straight lines which meet at the origin).

Returning to Figure 2, an important difference between type 1 and type 2 circles is shown by the angles ϕ_1 and ϕ_2, which the radial arm to the observed (Z_{xy}, Z_{xx}) or (Z_{xy}, Z_{yy}) data pair makes with the line joining the origin of axes to the circle center. For a type 1 circle, from Figure 2 note that ϕ_1 is given by

$$\phi_1 = \gamma - \beta \tag{40}$$

$$= 2\theta_e, \tag{41}$$

remembering equations (38) and (39), while for a type 2 circle,

$$\phi_2 = \gamma + \beta \tag{42}$$

$$= -2\theta_h. \tag{43}$$

Thus plotting type 1 circles will immediately display constancy of θ_e with period, and such is the case for the examples shown in the companion paper (Lilley, 1998). Constancy of θ_h with period would be most directly displayed by plotting type 2 circles.

In Figure 2, the angles θ_e and θ_h now have a physical expression, as also do the angles β, β', γ, and θ'.

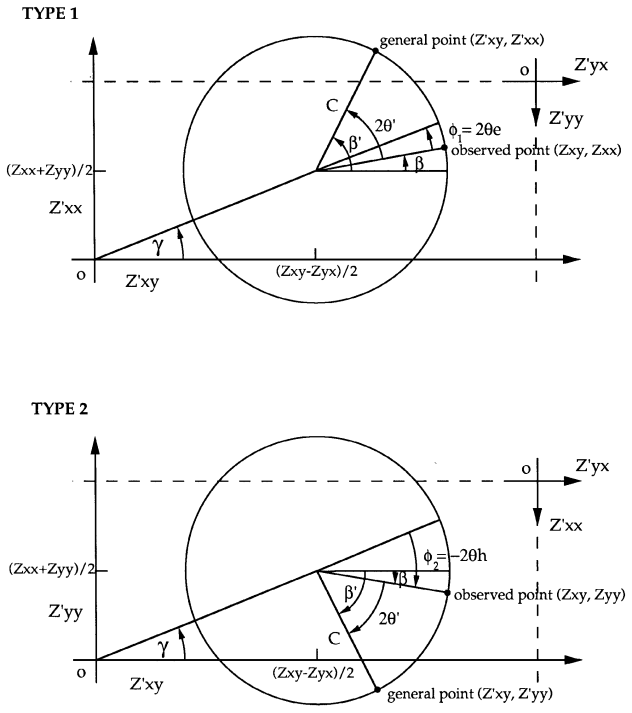

FIG. 2. The two basic arrangements for depicting MT matrix rotation with a circle, according to equations (29) to (32). The axes are Z'_{xy} (abscissa), with Z'_{xx} (ordinate) in type 1 and Z'_{yy} (ordinate) in type 2. C denotes radius of the circle. Note the ability to include axes for the other matrix elements on the diagrams. The sense in which an angle is measured positive from zero is indicated by the arrow on its arc. In the examples shown, $\theta_e = 5^\circ$ and $\theta_h = -16^\circ$.

Invariants with rotation of the measuring axes

Equations (29) to (32) show that $(Z'_{xx} + Z'_{yy})$ and $(Z'_{xy} - Z'_{yx})$ are independent of θ', and so are invariant with rotation of the measuring axes. Hence angle γ is also an invariant, as is the "central impedance," the distance from the origin of axes to the circle center (Lilley, 1993a). Denoting the central impedance by Z^L, its value is given by

$$Z^L = \tfrac{1}{2}\left[(Z_{xx} + Z_{yy})^2 + (Z_{xy} - Z_{yx})^2\right]^{\frac{1}{2}}. \tag{44}$$

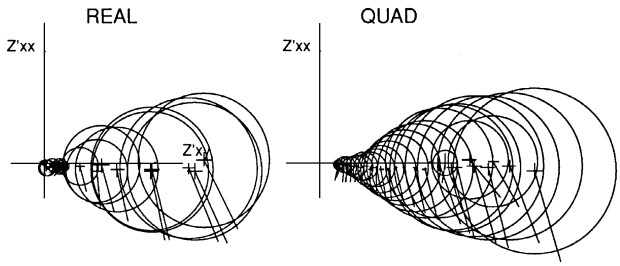

FIG. 3. An example (PNG103) of 2-D data, from the PNG data set distributed for the MTDIW2 meeting (Jones and Schultz, 1997). The radial arms of the circles intersect the circles at the actual observed points. These data also show static shift (Lilley, 1993b, 1997).

Another invariant is the quantity C. By adding equations (30) and (31) and squaring the result, subtracting equations (29) and (32) and squaring the result, then summing the two squared equations, it follows that in addition to equation (33), C may also be expressed as

$$C = \tfrac{1}{2}\left[(Z'_{xx} - Z'_{yy})^2 + (Z'_{xy} + Z'_{yx})^2\right]^{\frac{1}{2}}. \quad (45)$$

In fact, it is evident from Figure 2 that these quantities and several others are invariant. It can be seen that there are several sets of invariants which can be used to define a magnetotelluric impedance tensor. From inspection of Figure 2, one straightforward set can be seen to be:

1) Z^L, the distance from the origin of axes to the circle center, which gives the 1-D "scale" of a matrix, and is its 1-D kernel.
2) λ, an angle which gives a measure of the two dimensionality or anisotropy of a matrix, defined as

$$\lambda = \arcsin(C/Z^L). \quad (46)$$

3) γ, an angle which gives a measure of the three dimensionality of a matrix.

Z^L, λ, and γ will have values for both the real and quadrature matrices of the tensor, and thus comprise six invariants.

A seventh invariant, which is a further parameter of three dimensionality, links the real and quadrature parts of a tensor and may be expressed as

$$\delta\beta = \beta_r - \beta_q, \quad (47)$$

where β_r and β_q refer to the values of β for the real and quadrature parts of a tensor, respectively. By equation (38),

$$\delta\beta = \theta_{eq} - \theta_{er} + \theta_{hq} - \theta_{hr}. \quad (48)$$

These invariants, Z_r^L, λ_r, γ_r, Z_q^L, λ_q , γ_q, and $\delta\beta$, are shown in Figure 4.

An exploratory use of these invariants to quantify three dimensionality was made by Lilley and Corkery (1993). Recently, Fischer and Masero (1994) and Szarka and Menvielle (1997) discussed the question of specifying an MT tensor on the basis of its invariants. Earlier papers are by Ingham (1988) and Park and Livelybrooks (1989).

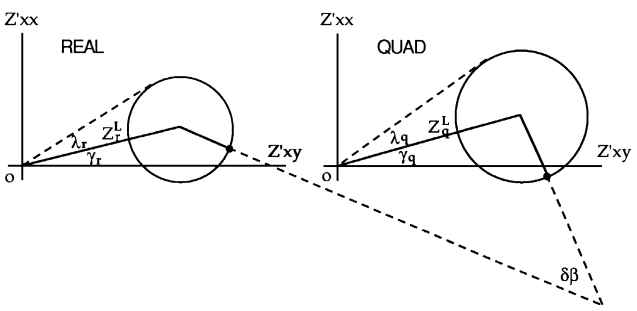

FIG. 4. A pair of real and quadrature circles for a tensor, showing the set of invariants Z_r^L, λ_r, γ_r, Z_q^L, λ_q, γ_q, and $\delta\beta$ by which the complete tensor may be specified.

A fundamental criterion

As shown in Figure 2, generally the circumference of a Mohr circle representing an MT matrix will not enclose the origin of the axes. In the terms of Figure 2, for a 1-D case the circle will reduce to a point on the horizontal axis. For a 2-D case, the circle will be centered on the horizontal axis, and it will cut the horizontal axis at two values of the same sign (both positive for the real part of the tensor) representing two principal impedances. For a 3-D case, the circle center will move off the axis, and for highly anisotropic data (either 2-D or 3-D), the circumference of the circle will approach the origin of the axes (Lilley, 1993a). Within the scope of the present paper, however, no physical circumstances arise which cause the radius of a circle to increase in such a way that the circumference encloses the origin of the axes.

A fundamental criterion is thus introduced. The requirement that a circle not enclose the origin of the axes may be expressed as the circle radius C being less than the central impedance Z^L. The inequality

$$C < Z^L \quad (49)$$

may be reduced to

$$Z_{xy}Z_{yx} < Z_{xx}Z_{yy}, \quad (50)$$

and observed tensor data which do not meet this criterion (in either real or quadrature part, or both) are flagged as invalid for later determining minor principal impedance values, following the techniques of the present paper.

ANALYSIS IN TERMS OF ELEMENTS OF STRUCTURAL GEOLOGY

The characteristics of MT impedance tensors may be analyzed in terms of models in which general operators have been applied to matrices of standard (1-D, 2-D, and 3-D) form. If a general operator applied to a standard matrix produces a new matrix with characteristics the same as an observed tensor, then a possibly helpful decomposition of the observed tensor has been found. Such an analysis is first a mathematical step; a subsequent step is to seek a reasonable physical and geological interpretation (if one exists) of such operators.

In this paper, following Means (1994) use of such operators in structural geology, just two matrix operators will be introduced: twist and split. In the magnetotelluric case, twist is the rotation of one (or both unequally) of the electric and magnetic fields at the point of observation, as in Figure 1a (note that twist is distinct from a regular rotation of the measuring axes, which involves the rotation of both the electric and magnetic fields equally, as in Figure 1b).

The split operator is the pure shear operator of Means (1990), also sometimes known as the stretching operator. In structural geology, it involves shear deformation only, without any inherent twist. It is thus to be distinguished from the shear operator as used by Groom and Bailey (1989), which does involve an inherent twist, resulting from the shear axes being at 45° to the main axes. In fact the Groom-Bailey shear operator is not included in the present treatment because it is not required for the most basic tensor decompositions. Otherwise, the twist and split operators introduced here are the same as the Groom-Bailey twist and split operators (the Groom-Bailey

nomenclature is used intentionally). In the magnetotelluric case, as will be shown, a standard 2-D impedance can be parametrized as a "split 1-D" impedance.

Different operators can be considered to have been applied in succession to produce an MT matrix as now observed. The order of application of the operators is important because they do not commute, and generally each successive operator will cause the history of the MT matrix to become increasingly complicated and difficult to interpret. After introducing the twist and split operators graphically, this paper takes the approach of examining the most simple histories possible, of which there are two: split after twist, and twist after split.

THE SPLITTING OPERATOR

Split operating on a 1-D matrix: the simplest cause of two dimensionality

Take a splitting operator

$$\begin{bmatrix} 1+S & 0 \\ 0 & 1-S \end{bmatrix}, \tag{51}$$

where S is the parameter defining the extent of the splitting, and imagine it applied to a 1-D matrix

$$\begin{bmatrix} 0 & 1 \\ -1 & 0 \end{bmatrix} Z_{12} \tag{52}$$

to give

$$\begin{bmatrix} 1+S & 0 \\ 0 & 1-S \end{bmatrix} \begin{bmatrix} 0 & 1 \\ -1 & 0 \end{bmatrix} Z_{12} \tag{53}$$

$$= \begin{bmatrix} 0 & 1+S \\ -(1-S) & 0 \end{bmatrix} Z_{12} \tag{54}$$

A 2-D matrix can thus be interpreted in terms of a splitting operator very directly, and indeed can be "desplit" (within the terms of the model). In equation (54), the original 1-D impedance value is given by the average impedance for the split 2-D matrix, i.e., by the value $(Z_{xy} - Z_{yx})/2$, which is recognized as the Berdichevsky average impedance (Berdichevsky and Dmitriev, 1976; Hobbs, 1992).

Note that application of the splitting operator has not caused any twisting of the matrix, and that the axes of the splitting operator have defined the principal axis directions of the new 2-D matrix. Mohr circles of both types for the matrix on the right-hand side of equation (54) are shown in Figure 5.

Split operating on a 2-D matrix

The splitting operator in the previous section may also be considered to act on a matrix which is already 2-D. Generally, the strike direction of the 2-D matrix will not coincide with the splitting direction, so that the 2-D matrix may be cast in the form

$$\begin{bmatrix} C\sin\beta' & Z_4 + C\cos\beta' \\ -Z_4 + C\cos\beta' & -C\sin\beta' \end{bmatrix}, \tag{55}$$

where equations (29) to (32) have been invoked, and it has been remembered that for a 2-D case

$$Z_{xx} + Z_{yy} = 0. \tag{56}$$

Also, notation Z_4 has been introduced for

$$Z_4 = (Z_{xy} - Z_{yx})/2. \tag{57}$$

The splitting operator applied to matrix (55) gives

$$\begin{bmatrix} 1+S & 0 \\ 0 & 1-S \end{bmatrix} \begin{bmatrix} C\sin\beta' & Z_4 + C\cos\beta' \\ -Z_4 + C\cos\beta' & -C\sin\beta' \end{bmatrix} \tag{58}$$

$$= \begin{bmatrix} C\sin\beta'(1+S) & (Z_4 + C\cos\beta')(1+S) \\ (-Z_4 + C\cos\beta')(1-S) & -C\sin\beta'(1-S) \end{bmatrix}. \tag{59}$$

This latter matrix (59) produces Mohr circles of type 1 and type 2 with characteristics as shown in Figure 5.

A split operator applied to a general 2-D matrix has thus produced 3-D circles, seen as off-axis in Figure 5. The possibility is demonstrated that a 3-D matrix may be decomposed in terms of a split acting on a 2-D matrix. This possible decomposition is not pursued further here because of the number of parameters involved. Zhang et al. (1987), however, treat this case, for the situation in which the distortion of the real and quadrature parts of an impedance tensor is the same.

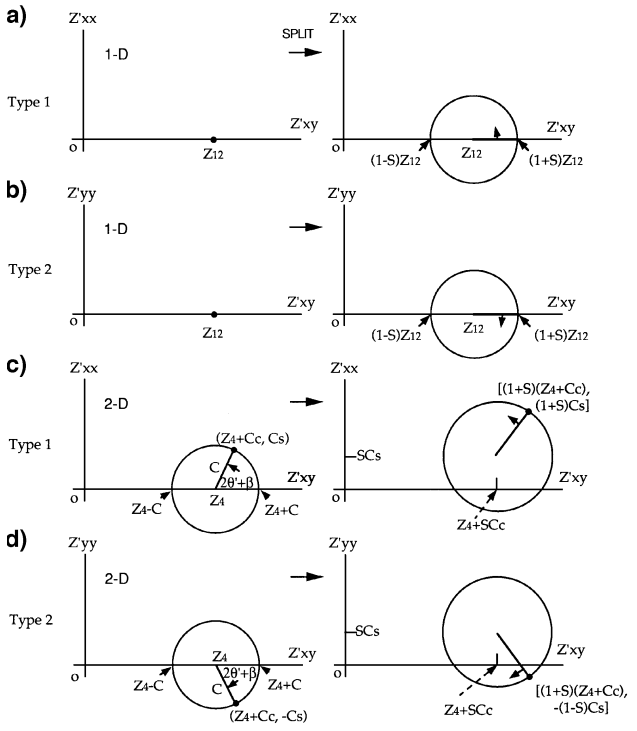

FIG. 5. Effects of a splitting operator on 1-D cases (a and b) and 2-D cases (c and d) for both type 1 and type 2 diagrams. The left-hand and right-hand columns are before and after application of the splitting operator. Here c and s denote $\cos\beta'$ and $\sin\beta'$, respectively.

In the present paper, remembering that infinitely many combinations of the operators are possible, attention will now focus on the fundamental twist-after-split and split-after-twist combinations.

TWIST: THE SIMPLEST CAUSE OF THREE DIMENSIONALITY

Taking Mohr circles for a general matrix as in Figure 2, twist operators will be applied. It will be shown that now a major difference becomes apparent between the two types of circle in the relative movement of the radial arm. In the type 1 circle, the radial arm rotates counter to the rotation of the line joining the circle center to the origin of the axes. In the type 2 circle, the radial arm rotates sympathetic with the line joining the circle center to the origin of the axes. These characteristics produce diagnostic Mohr diagrams, which will be useful in the analysis of observed data.

Taking the general matrix of equation (1), a twist is applied to it of form

$$\begin{bmatrix} \cos\psi & \sin\psi \\ -\sin\psi & \cos\psi \end{bmatrix}. \tag{60}$$

This expression for twist is the same as that of rotation of just the E axes in equation (6). Indeed, the twist can be thought of as a rotation of the electric field only counterclockwise through angle ψ, or as a rotation of the magnetic field only clockwise through angle ψ.

The result of application of the twist is thus

$$\begin{bmatrix} \cos\psi & \sin\psi \\ -\sin\psi & \cos\psi \end{bmatrix} \begin{bmatrix} Z_{xx} & Z_{xy} \\ Z_{yx} & Z_{yy} \end{bmatrix} \tag{61}$$

$$= \begin{bmatrix} \cos\psi Z_{xx} + \sin\psi Z_{yx} & \cos\psi Z_{xy} + \sin\psi Z_{yy} \\ -\sin\psi Z_{xx} + \cos\psi Z_{yx} & -\sin\psi Z_{xy} + \cos\psi Z_{yy} \end{bmatrix}, \tag{62}$$

resulting in Mohr diagrams as shown in Figure 6, from the original circles shown in Figure 2. Note that γ', the new γ angle, is given for both type 1 and type 2 circles by

$$\tan\gamma' = \frac{\cos\psi(Z_{xx} + Z_{yy}) - \sin\psi(Z_{xy} - Z_{yx})}{\cos\psi(Z_{xy} - Z_{yx}) + \sin\psi(Z_{yy} + Z_{xx})} \tag{63}$$

$$= \tan(\gamma - \psi) \tag{64}$$

by equation (37). Hence, the applied twist of angle ψ is directly shown for circles of both types 1 and 2 as a clockwise rotation by ψ of the line joining the origin of the axes to the circle center.

For the type 1 circle, the new angle ϕ_1' (after some algebra) is given by

$$\phi_1' = \phi_1 - 2\psi, \tag{65}$$

indicating that as the line from the origin to the circle center rotates by ψ clockwise, the radius of the circle to the observed point counterrotates angle 2ψ.

For the type 2 circle, however, the new angle ϕ_2' is given by

$$\phi_2' = \phi_2, \tag{66}$$

so that the twist operator leaves the angle ϕ_2 on a type 2 diagram unchanged.

Substitution of the appropriate values from the right-hand side of equation (62) into equations (33) and (44) shows that application of twist has not changed the radius of the circle, nor the distance from the origin to the circle center.

Thus, applying these results in reverse, general 3-D matrices in both type 1 and type 2 diagrams, as in Figure 2, may be reduced to 2-D matrices by the application of an appropriate "detwisting" angle ψ. Both type 1 and type 2 diagrams will swing down so that their centers locate on the horizontal axis; the difference being that type 2 diagrams will keep fixed the angle ϕ_2, whereas in type 1 diagrams, ϕ_1 will change by a counterrotation of the radial arm by 2ψ.

THE SIMPLEST DECOMPOSITION PATHS

Two paths

The Means (1994) summary of the two basic ways in which finite deformation in a rock material can be factorized into components of twist and pure shear (one where pure shear premultiplies twist, the other where pure shear postmultiplies twist) suggests also the two most simple basic paths for producing a 3-D tensor in magnetotellurics. In the terminology of this paper where "split" is used for pure shear, these two paths are split after twist and twist after split.

Taken in reverse, these paths are tensor decomposition paths. An actual data set can be decomposed, mathematically, by both paths. Whereas both paths will give the same results for the

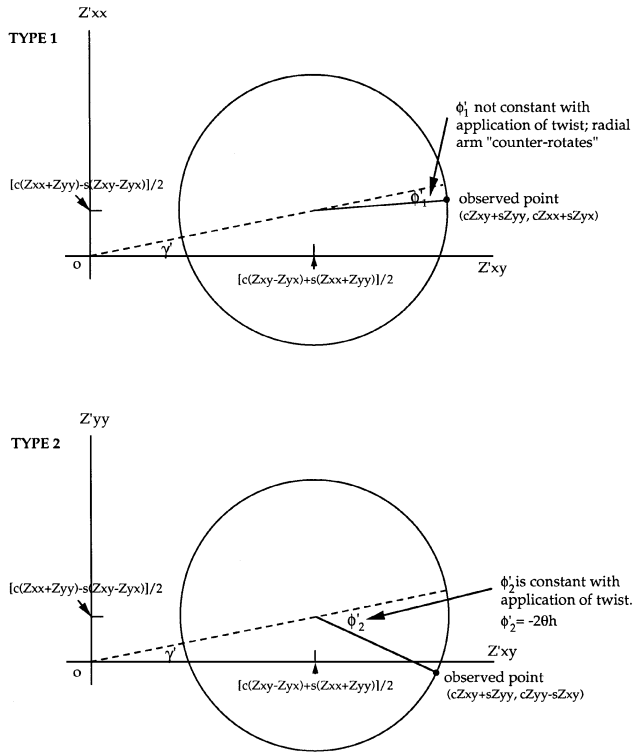

FIG. 6. The effects of a twist operator on diagrams of type 1 and type 2 (as described in the section on twist). Here c and s denote $\cos\psi$ and $\sin\psi$, where ψ is the additional twist applied to the general cases of Figure 2.

twist angle and for the value of the split, the different paths will give different results for the split direction.

Path 1: split after twist

Imagine a 1-D matrix,

$$\begin{bmatrix} 0 & 1 \\ -1 & 0 \end{bmatrix} Z_{12}, \tag{67}$$

upon which a twist through angle ψ

$$\begin{bmatrix} \cos\psi & \sin\psi \\ -\sin\psi & \cos\psi \end{bmatrix} \tag{68}$$

operates, to give the result

$$\begin{bmatrix} \cos\psi & \sin\psi \\ -\sin\psi & \cos\psi \end{bmatrix} \begin{bmatrix} 0 & 1 \\ -1 & 0 \end{bmatrix} Z_{12} \tag{69}$$

$$= \begin{bmatrix} -\sin\psi & \cos\psi \\ -\cos\psi & -\sin\psi \end{bmatrix} Z_{12}. \tag{70}$$

The twist could be caused, for instance, by the electric field being twisted counterclockwise through angle ψ.

Now imagine application of a splitting operator

$$\begin{bmatrix} 1+S & 0 \\ 0 & 1-S \end{bmatrix} \tag{71}$$

to give

$$\begin{bmatrix} 1+S & 0 \\ 0 & 1-S \end{bmatrix} \begin{bmatrix} -\sin\psi & \cos\psi \\ -\cos\psi & -\sin\psi \end{bmatrix} Z_{12} \tag{72}$$

$$= \begin{bmatrix} -\sin\psi(1+S) & \cos\psi(1+S) \\ -\cos\psi(1-S) & -\sin\psi(1-S) \end{bmatrix} Z_{12}. \tag{73}$$

That is, in this case,

$$Z_{xx} = -\sin\psi(1+S)Z_{12}, \tag{74}$$

$$Z_{xy} = +\cos\psi(1+S)Z_{12}, \tag{75}$$

$$Z_{yx} = -\cos\psi(1-S)Z_{12}, \tag{76}$$

$$Z_{yy} = -\sin\psi(1-S)Z_{12}, \tag{77}$$

and with these values equations (33) and (34) give

$$C = SZ_{12} \tag{78}$$

and

$$\tan\beta = -\tan\psi. \tag{79}$$

For both type 1 and type 2 diagrams, this path is shown in Figure 7a.

Any observed matrix of elements Z'_{xx}, Z'_{xy}, Z'_{yx}, and Z'_{yy} may thus be interpreted in terms of this split-after-twist model. The four observed parameters give four model parameters: Z_{12}, ψ, S, and θ'. Such an interpretation is a direct and indeed unique decomposition of the observed matrix, taking the split-after-twist path in reverse.

The parameters Z_{12}, ψ, S, and θ' have the uses that Z_{12} gives a basic scale for the impedance magnitude, ψ is a parameter of three dimensionality, S is a measure of two dimensionality, and θ' relates the 2-D strike to the measuring axes. In expression (72), the simple form used for the splitting operator carries the implication that splitting is aligned with the reference axes; this in turn carries the implication (as splitting is being taken to parametrise geological two dimensionality) that the axes for 2-D structure are those of the reference axes.

Angle θ' is the angle of rotation of the observing axes clockwise from the axes in which equations (74) to (77) are set up. Thus, the direction of geologic strike will be θ' counterclockwise from the axes in which Z'_{xx}, Z'_{xy}, Z'_{yx}, and Z'_{yy} are measured.

To obtain the four parameters of the decomposition model, θ' is determined using equations (35) and (36), i.e.,

$$\theta' = \frac{1}{2}\left[\arctan\frac{Z'_{xx} - Z'_{yy}}{Z'_{xy} + Z'_{yx}} - \beta\right] \tag{80}$$

$$= \frac{1}{2}\left[\arctan\frac{Z'_{xx} - Z'_{yy}}{Z'_{xy} + Z'_{yx}} - \arctan\frac{Z'_{xx} + Z'_{yy}}{Z'_{xy} - Z'_{yx}}\right], \tag{81}$$

noting that $-\tan\psi$ is given by

$$\frac{Z'_{xx} + Z'_{yy}}{Z'_{xy} - Z'_{yx}} = \frac{Z_{xx} + Z_{yy}}{Z_{xy} - Z_{yx}} = -\tan\psi \tag{82}$$

and using equation (79). Z_{12} and S may be determined from a knowledge of SZ_{12} [using equations (78) and (45)], and the value for Z_{12} given by

$$Z_{12} = \tfrac{1}{2}\left[(Z'_{xx} + Z'_{yy})^2 + (Z'_{xy} - Z'_{yx})^2\right]^{\frac{1}{2}}. \tag{83}$$

Equation (83) can be confirmed using equations (74) to (77), plus the knowledge that $(Z'_{xx} + Z'_{yy})$ and $(Z'_{xy} - Z'_{yx})$ are both invariants with the rotation of axes. Z_{12}, as in equation (83), is in fact the central impedance [compare equation (44)].

Note that these solutions are the same as in the basic theorem at the start of this paper, allowing for the equivalence of the different notations, with

$$\theta' = -\theta_e, \tag{84}$$

i.e., the direction of the E field splitting axis, also taken to be that of local geologic strike, is θ_e clockwise from the axes in which Z'_{xx}, Z'_{xy}, Z'_{yx}, and Z'_{yy} are measured.

Path 2: twist after split

Now imagine the above procedure to occur in the other order. A 1-D matrix,

$$\begin{bmatrix} 0 & 1 \\ -1 & 0 \end{bmatrix} Z_{12}, \tag{85}$$

is acted on by a splitting operator

$$\begin{bmatrix} 1+S & 0 \\ 0 & 1-S \end{bmatrix} \tag{86}$$

to give

$$\begin{bmatrix} 1+S & 0 \\ 0 & 1-S \end{bmatrix} \begin{bmatrix} 0 & 1 \\ -1 & 0 \end{bmatrix} Z_{12} \tag{87}$$

$$= \begin{bmatrix} 0 & 1+S \\ -(1-S) & 0 \end{bmatrix} Z_{12}, \tag{88}$$

and the whole is than acted on by a twist

$$\begin{bmatrix} \cos\psi & \sin\psi \\ -\sin\psi & \cos\psi \end{bmatrix} \tag{89}$$

to give

$$\begin{bmatrix} \cos\psi & \sin\psi \\ -\sin\psi & \cos\psi \end{bmatrix} \begin{bmatrix} 0 & 1+S \\ -(1-S) & 0 \end{bmatrix} Z_{12} \tag{90}$$

$$= \begin{bmatrix} -\sin\psi(1-S) & \cos\psi(1+S) \\ -\cos\psi(1-S) & -\sin\psi(1+S) \end{bmatrix} Z_{12}. \tag{91}$$

Thus, now

$$Z_{xx} = -\sin\psi(1-S)Z_{12}, \tag{92}$$

$$Z_{xy} = +\cos\psi(1+S)Z_{12}, \tag{93}$$

$$Z_{yx} = -\cos\psi(1-S)Z_{12}, \tag{94}$$

$$Z_{yy} = -\sin\psi(1+S)Z_{12}. \tag{95}$$

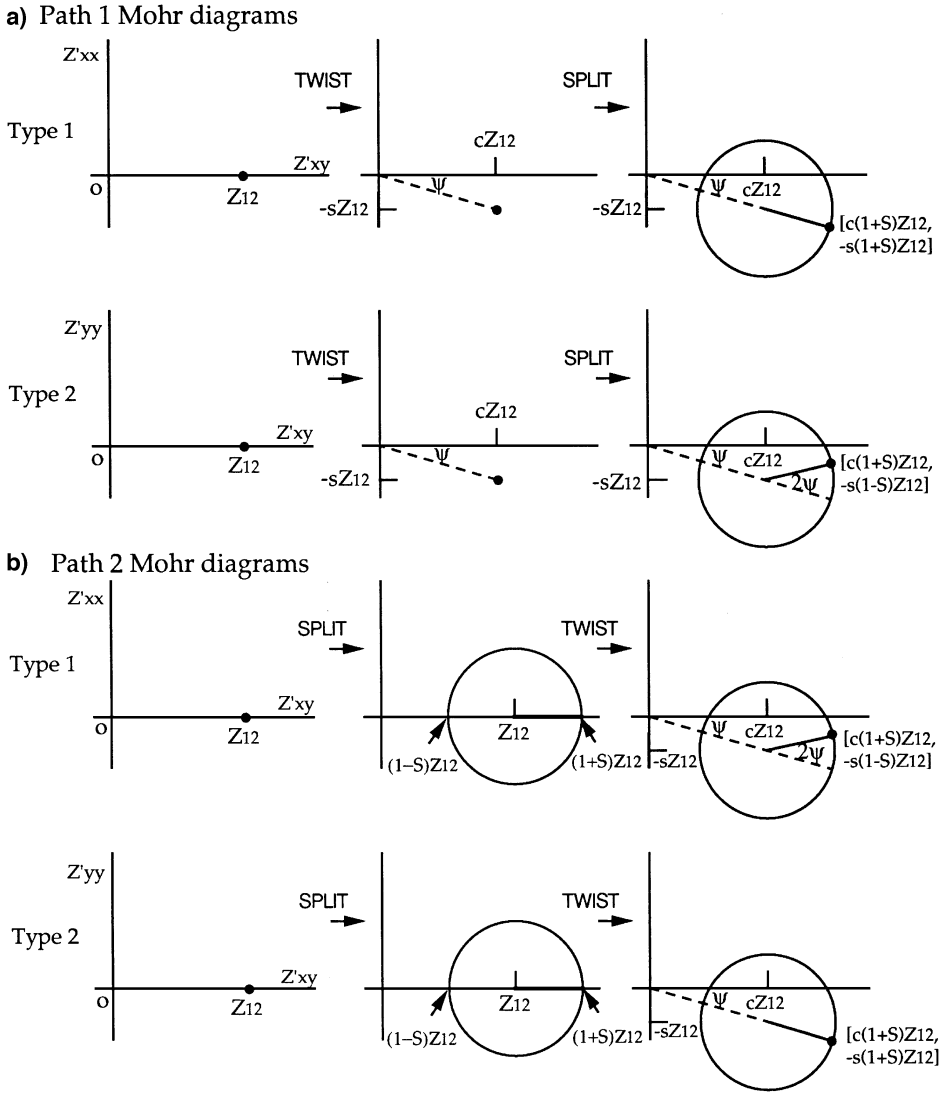

FIG. 7. Mohr diagrams for paths 1 and 2. Here c and s denote $\cos\psi$ and $\sin\psi$, where ψ is the twist.

Path 2 is also shown, for both type 1 and type 2 circles, in Figure 7b. This path may also be taken in reverse to achieve a tensor decomposition in terms of the parameters Z_{12}, ψ, S, and θ'. Again,

$$C = SZ_{12} \tag{96}$$

and

$$\frac{Z'_{xx} + Z'_{yy}}{Z'_{xy} - Z'_{yx}} = \frac{Z_{xx} + Z_{yy}}{Z_{xy} - Z_{yx}} = -\tan\psi, \tag{97}$$

though note now that [from equation (34)]

$$\tan\beta = +\tan\psi, \tag{98}$$

so that θ' becomes

$$\theta' = \frac{1}{2}\left[\arctan\frac{Z'_{xx} - Z'_{yy}}{Z'_{xy} + Z'_{yx}} + \arctan\frac{Z'_{xx} + Z'_{yy}}{Z'_{xy} - Z'_{yx}}\right] \tag{99}$$

$$= -\theta_h. \tag{100}$$

This result is consistent with the application of the split operator to the MT tensor in expression (87), before application of the twist operator. The simple form taken for the split operator implies that the 2-D structure is aligned with the reference axes, before application of the twist. As it is the E field which is twisted, the H field maintains the direction of the geologic strike.

Comparison with results of the basic theorem

A comparison of the results of the previous two sections with those of the introductory theorem shows that the two basic 2-D decompositions give a formal basis to the earlier intuitive interpretation of θ_e, θ_h, Z^P_{xy}, and Z^P_{yx}. These parameters are confirmed as fundamental in the 2-D analysis of a general MT tensor. In particular, the split-after-twist decomposition gives the E axis as the splitting direction, after a twist from the H-axis direction; the twist-after-split decomposition gives the H axis as the splitting direction, and then a twist to the E-axis direction.

Both decompositions give the same principal values as in equations (26) and (27), the split-after-twist decomposition attributing these values to the E-axis split; the twist-after-split decomposition attributing the values to the H-axis split.

Note that the split parameter, S, is related to the anisotropy measure λ by

$$\lambda = \arcsin S \tag{101}$$

[compare equation (46)], where in Figure 7, all circles subtend angles of 2λ at their origin of axes.

CONCLUSIONS

Two simple MT matrix decompositions, in terms of the elements of twisting and splitting (pure shear), have been linked to a basic theorem for reducing a 3-D matrix to 2-D form by allowing the E and H observing axes to rotate independently. Common expressions for local strike (interpreted as the E-axis direction), regional strike (interpreted as the H-axis direction), and the two principal 2-D impedances are given by all these approaches.

Regarding the use of Mohr circles for magnetotelluric analysis, this paper has demonstrated how they may be used as a map or chart for decomposition. Field observations produce a matrix which may be brought on to the chart as a circle with particular characteristics. Once decomposed, the matrix may be taken from the chart again, as a circle with different characteristics, for the next step in data inversion and interpretation.

The decomposition process takes place on the chart, and how the matrix circle changes from its initial characteristics to its decomposed characteristics should be clear and easily understandable.

Finally, although this paper has dealt with decomposing actual 3-D data to 2-D form, the theory may also be useful in following the strategy of taking the model to the data as espoused by DeGroot-Hedlin (1995). In that strategy, computed 2-D models are distorted to match 3-D data, the distortions being part of the solution.

Under this approach, the most simple distorting factors may be the most useful, and it is these which are employed in this paper. The parameters of distortion to produce a given 3-D tensor from its nearest 2-D model may be expressed directly and uniquely.

SUMMARY OF FORMULAS FOR BASIC 2-D DECOMPOSITION

For clarity and ease of reference, the key equations derived above are collected here together and written in full with subscript r for real, and q for quadrature.

The observed tensor is

$$\begin{bmatrix} Z_{xx_r} + iZ_{xx_q} & Z_{xy_r} + iZ_{xy_q} \\ Z_{yx_r} + iZ_{yx_q} & Z_{yy_r} + iZ_{yy_q} \end{bmatrix}. \tag{102}$$

The twist is

$$\gamma_r = \arctan\left[\frac{Z_{yy_r} + Z_{xx_r}}{Z_{xy_r} - Z_{yx_r}}\right], \tag{103}$$

$$\gamma_q = \arctan\left[\frac{Z_{yy_q} + Z_{xx_q}}{Z_{xy_q} - Z_{yx_q}}\right], \tag{104}$$

and the criterion that the circumference of a circle should not enclose its origin of the axes is

$$Z_{xy_r} Z_{yx_r} < Z_{xx_r} Z_{yy_r}, \tag{105}$$

$$Z_{xy_q} Z_{yx_q} < Z_{xx_q} Z_{yy_q}. \tag{106}$$

The principal values are

$$Z^P_{xy_r} = \tfrac{1}{2}\left\{\left[Z_{yy_r} + Z_{xx_r}\right]^2 + \left[Z_{yx_r} - Z_{xy_r}\right]^2\right\}^{1/2} - \left\{\left[Z_{yy_r} - Z_{xx_r}\right]^2 + \left[Z_{xy_r} + Z_{yx_r}\right]^2\right\}^{1/2}, \tag{107}$$

$$Z^P_{xy_q} = \tfrac{1}{2}\left\{\left[Z_{yy_q} + Z_{xx_q}\right]^2 + \left[Z_{yx_q} - Z_{xy_q}\right]^2\right\}^{1/2} - \left\{\left[Z_{yy_q} - Z_{xx_q}\right]^2 + \left[Z_{xy_q} + Z_{yx_q}\right]^2\right\}^{1/2}, \tag{108}$$

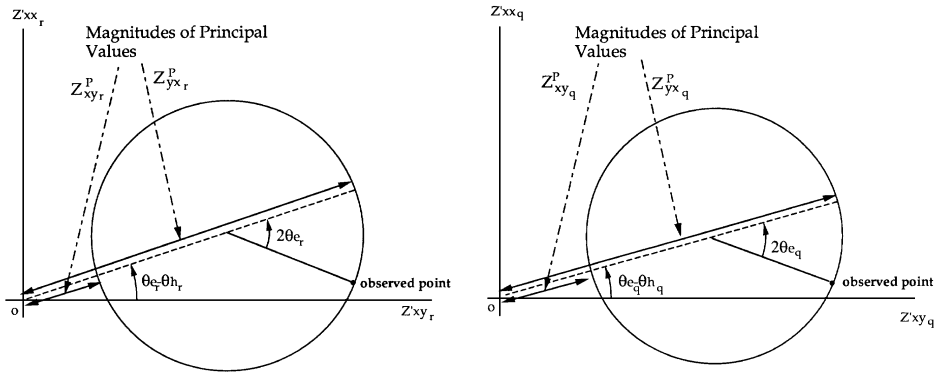

FIG. 8. Diagram showing the decomposition parameters θ_{er}, θ_{hr}, θ_{eq}, and θ_{hq} and the magnitudes of the principal values $Z^P_{xy_r}$, $Z^P_{yx_r}$, Z^P_{xyq}, and Z^P_{yxq} on a type 1 diagram. This diagram also shows how a circle that (due to error) encloses the origin will be invalid for the determination of a minor principal value.

and

$$Z^P_{yx_r} = \tfrac{1}{2}\left\{\left|Z_{yy_r} + Z_{xx_r}\right|^2 + \left|Z_{yx_r} - Z_{xy_r}\right|^2\right\}^{1/2} + \left\{\left|Z_{yy_r} - Z_{xx_r}\right|^2 + \left|Z_{xy_r} + Z_{yx_r}\right|^2\right\}^{1/2}, \quad (109)$$

$$Z^P_{yxq} = \tfrac{1}{2}\left\{\left|Z_{yyq} + Z_{xxq}\right|^2 + \left|Z_{yxq} - Z_{xyq}\right|^2\right\}^{1/2} + \left\{\left|Z_{yyq} - Z_{xxq})^2\right|^2 + \left|Z_{xyq} + Z_{yxq}\right|^2\right\}^{1/2}. \quad (110)$$

The direction of E-axis strike, reasonably interpreted as the direction of local geologic strike is

$$\theta_{er} = \frac{1}{2}\left\{\arctan\frac{Z_{yy_r} - Z_{xx_r}}{Z_{xy_r} + Z_{yx_r}} + \arctan\frac{Z_{yy_r} + Z_{xx_r}}{Z_{xy_r} - Z_{yx_r}}\right\}, \quad (111)$$

$$\theta_{eq} = \frac{1}{2}\left\{\arctan\frac{Z_{yyq} - Z_{xxq}}{Z_{xyq} + Z_{yxq}} + \arctan\frac{Z_{yyq} + Z_{xxq}}{Z_{xyq} - Z_{yxq}}\right\}. \quad (112)$$

The direction of H-axis strike, possibly interpreted as the direction of regional geologic strike, is

$$\theta_{hr} = \frac{1}{2}\left\{\arctan\frac{Z_{yy_r} - Z_{xxr}}{Z_{xy_r} + Z_{yx_r}} - \arctan\frac{Z_{yy_r} + Z_{xxr}}{Z_{xy_r} - Z_{yx_r}}\right\}, \quad (113)$$

$$\theta_{hq} = \frac{1}{2}\left\{\arctan\frac{Z_{yy_q} - Z_{xxq}}{Z_{xy_q} + Z_{yx_q}} - \arctan\frac{Z_{yy_q} + Z_{xxq}}{Z_{xy_q} - Z_{yx_q}}\right\}. \quad (114)$$

The angles θ_{er}, θ_{hr}, θ_{eq}, and θ_{hq} are measured clockwise from the orthogonal axes relative to which the tensor has been observed. The relationships between the key set of quantities θ_{er}, θ_{hr}, θ_{eq}, and θ_{hq} and the principal values $Z^P_{xy_r}$, $Z^P_{yx_r}$, $Z^P_{xy_q}$, and $Z^P_{yx_q}$ are summarised in Figure 8.

The above equations illustrate how the "two-mode" convention applies, so that the given quantities may be computed on a period-by-period basis for both real and quadrature modes. For angles, the real and quadrature mode values may then be averaged. For the principal impedances, the real and quadrature principal values may be combined to give complex impedance values; these correspond to recognizing that the real and quadrature parts of a tensor are affected by different degrees of twist.

ACKNOWLEDGMENTS

I thank many people for discussing the ideas central to this paper, including Professor R. Mereu, whose lecture on Mohr circles I remembered years later when addressing the analysis of another tensor, and Professor W. Means, whose discussions helped my understanding of the characteristics such circles displayed for MT data. I thank Alan Jones for initiating and leading the MTDIW workshops of 1992 and 1994; I thank others at the meetings for their discussion. I have benefitted recently from discussion with Ian Ferguson, Graham Heinson, Alan Chave, Liejun Wang, Malcolm Ingham, and John Weaver. The comments of Associate Editors and referees have added greatly to this paper.

REFERENCES

Bahr, K., 1988, Interpretation of the magnetotelluric impedance tensor: Regional induction and local telluric distortion: J. Geophys., **62**, 119–127.

——— 1991, Geological noise in magnetotelluric data: A classification of distortion types: Phys. Earth Planet. Internat. **66**, 24–38.

Berdichevsky, M. N., and Dmitriev, V. I., 1976, Basic principles of interpretation of magnetotelluric curves, *in* Adam, A., Ed., Geoelectric and geothermal studies: Akademiai Kaido Budapest, KAPG Geophys. Mono., 165–221.

Chakridi, R., Chouteau, M., and Mareschal, M., 1992, A simple technique for analysing and partly removing galvanic distortion from the magnetotelluric impedance tensor: Application to Abitibi and Kapuskasing data: Geophys. J. Internat., **108**, 917–929.

Chave, A. D., and Smith, J. T., 1994, On electric and magnetic galvanic distortion tensor decompositions: J. Geophys. Res., **99**, 4669–4682.

Cox, C. S., Filloux, J. H., Gough, D. I., Larsen, J. C., Poehls, K. A., Von Herzen, R. P., and Winter, R., 1980, Atlantic lithospheric sounding: J. Geomag. Geoelectr., **32** , Supplement I, 13–32.

DeGroot-Hedlin, C., 1995, Inversion for regional 2-D resistivity structure in the presence of galvanic scatterers: Geophys. J. Internat., **122**, 877–888.

DePaor, D. G., and Means, W. D., 1984, Mohr circles of the first and second kind and their use to represent tensor operations: J. Struct. Geol., **6**, 693–701.

Ferguson, I. J., 1988, The Tasman project of seafloor magnetotelluric exploration: Ph.D. thesis, Australian National Univ.
Ferguson, I. J., Lilley, F. E. M., and Filloux, J. H., 1990, Geomagnetic induction in the Tasman Sea and electrical conductivity structure beneath the Tasman seafloor: Geophys. J. Internat., **102**, 299–312.
Fischer, G., and Masero, W., 1994, Rotational properties of the magnetotelluric impedance tensor: The example of the Araquainha impact crater, Brazil: Geophys. J. Internat., **119**, 548–560.
Groom, R. W., and Bailey, R. C., 1989, Decomposition of magnetotelluric impedance tensors in the presence of local three-dimensional galvanic distortion: J. Geophys. Res., **94**, 1913–1925.
Hobbs, B. A., 1992, Terminology and symbols for use in studies of electromagnetic induction in the Earth: Surveys in Geophys. **13,** 489–515.
Ingham, M. R., 1988, The use of invariant impedances in magnetotelluric interpretation: Geophys. J., **92**, 165–169.
Jones, A. G., and Schultz, A., 1997, Introduction to MT-DIW2 Special Issue: J. Geomag. Geoelectr., **49**, 727–737.
Larsen, J. C., 1975, Low frequency (0.1–6.0 cpd) electromagnetic study of deep mantle electrical conductivity beneath the Hawaiian Islands: Geophys. J., **43**, 17–46.
Lilley, F. E. M., 1976, Diagrams for magnetotelluric data: Geophysics, **41**, 766–770.
——— 1993a, Magnetotelluric analysis using Mohr circles: Geophysics, **58**, 1498–1506.
——— 1993b, Mohr circles in magnetotelluric interpretation (i) Simple static shift; (ii) Bahr's analysis: J. Geomag. Geoelectr., **45**, 833–839.
——— 1997, A critique of the MTDIW2-PNG data set based on Mohr circles: J. Geomag. Geoelectr., **49**, 807–815.
——— 1998, Magnetotelluric tensor decomposition: 2. Examples of a basic procedure: Geophysics, **63**, 1898–1907.
Lilley, F. E. M., and Arora, B. R., 1982, The sign convention for quadrature Parkinson arrows in geomagnetic induction studies: Rev. Geophys. Space Phys., **20**, 513–518.
Lilley, F. E. M., and Corkery, R. W., 1993, The Australian continent: A numerical model of its electrical conductivity structure, and electromagnetic response: Expl. Geophys., **24** 637–644.
Means, W. D., 1990, Kinematics, stress, deformation and material behavior: J. Struct. Geol., **12**, 953–971.
——— 1992. How to do anything with Mohr circles; A short course about tensors for structural geologists: State Univ. of New York at Albany.
——— 1994, Rotational quantities in homogeneous flow and the development of small-scale structure: J. Struct. Geol., **16**, 437–445.
Park, S. K., and Livelybrooks, D. W., 1989, Quantitative interpretation of rotationally invariant parameters in magnetotellurics: Geophysics, **54**, 1483–1490.
Parkinson, W. D., 1983, Introduction to geomagnetism: Scottish Academic Press.
Pedersen, L. B., 1988, Some aspects of magnetotelluric field procedures: Surveys in Geophys., **9**, 245–257.
Smith, J. T., 1995, Understanding telluric distortion matrices: Geophys. J. Internat., **122**, 219–226.
Szarka, L., and Menvielle, M., 1997, Analysis of rotational invariants of the magnetotelluric impedance tensor: Geophys. J. Internat., **129**, 133–142.
Weaver, J. T., 1994, Mathematical methods for geo-electromagnetic induction: Research Studies Press.
Zhang, P., Roberts, R. G., and Pedersen, L. B., 1987, Magnetotelluric strike rules: Geophysics, **51**, 267–278.

APPENDIX

SIGNS OF THE QUADRATURE TENSOR INVARIANTS $(Z'_{xy} - Z'_{yx})$ AND $(Z'_{xx} + Z'_{yy})$

$(Z'_{xy} - Z'_{yx})$

As noted in the section on general rotation of axes, the quantity $(Z'_{xy} - Z'_{yx})$ is an invariant with the rotation of axes, and it is evident from inspection of Figure 2 that $(Z'_{xy} - Z'_{yx})$ is always positive in the real mode.

In the quadrature mode, the sign of $(Z'_{xy} - Z'_{yx})$ will depend upon whether, earlier in the analysis, a time-dependence of $e^{+i\omega t}$ or $e^{-i\omega t}$ was assumed for the observed data. (Such an assumption is necessary in calculating complex values of Z'_{xy} and Z'_{yx} at frequency ω.)

When the time-series analysis adopts an $e^{+i\omega t}$ dependence, for example as in the theoretical development of Weaver (1994), then for induction in a half-space the phase angle is $+45^\circ$, and $(Z'_{xy} - Z'_{yx})$ should be positive in quadrature mode.

When the time-series analysis adopts an $e^{-i\omega t}$ dependence, for example in Parkinson (1983) and as recommended by Hobbs (1992), then $(Z'_{xy} - Z'_{yx})$ should be negative in quadrature mode. When $(Z'_{xy} - Z'_{yx})$ is negative, the center of the appropriate circle will plot to the left of the vertical axis, rather than to the right.

$(Z'_{xx} + Z'_{yy})$

The sign of the invariant $(Z'_{xx} + Z'_{yy})$ in real mode can be either positive or negative depending upon whether angle γ is positive or negative. Similarly, quadrature $(Z'_{xx} + Z'_{yy})$ can be of either sign.

Discussion

Changing from $e^{+i\omega t}$ to $e^{-i\omega t}$ time dependence causes changes of sign in the quadrature tensor elements, which are seen in the circles as a rotation of the E-field measuring axes through 180° (i.e., γ increases by 180°). The similar matter of the sign of quadrature induction arrows is discussed in Lilley and Arora (1982), where more details are given.

The examples in the companion paper (Lilley, 1998) all indicate use of $e^{+i\omega t}$ time dependence, as all quadrature mode circles have their centers to the right of the vertical axis. An example of $e^{-i\omega t}$ time dependence and circle centers left of the vertical axis is that of Figure 5 in Lilley (1993a), which quotes results from Ferguson (1988).

Finally, note again that although quadrature circle centers may be left or right of the vertical axis, in real mode the circle centers will always be to the right. Hence, a real-mode circle with center left of the vertical axis (as in Figure 1f of Lilley, 1976) suggests an error of procedure (in this case, thought to lie in the sign of the E-field calibration).